Spectral widths of H_2^+ multiphoton dissociation with short intense laser pulses

O. Atabek
Laboratoire de Photophysique Moléculaire du Centre National de la Recherche Scientifique, Bâtiment 213, Université Paris-Sud, 91405 Orsay Cedex, France

G. Jolicard
Laboratoire de Physique Moléculaire, Faculté des Sciences de Besançon, La Bouloie—Route de Gray, 25030 Besançon Cedex, France

(Received 2 June 1993)

Photodissociation spectra of H_2^+, obtained using ultrashort (a few femtoseconds), intense (within the range of 10^{12} to 10^{14} W/cm^2) laser pulses (with a peak frequency of 3.761 eV), and displaying well-separated proton kinetic-energy peaks corresponding to one-, two-, or three-photon absorptions are analyzed. Within some approximations, the validity range of which is related to the aforementioned assumptions on the laser and spectrum characteristics, a simple analytic formula is deduced. It gives the spectral widths of the observed peaks in terms of the total number of photons which are absorbed and/or emitted during the dissociation process. A quantitative support to some recent dynamical interpretations is provided. The successive absorption of three photons seems basically to be the initial step which, at intermediate intensities, leads to the three-photon peaks. A subsequent emission of one (or two) photons is responsible for the two- (or one-) photon peaks. Bond softening occurs at higher intensities by the lowering of potential-energy barriers. Dissociation proceeds through these barriers by reflection and tunneling. It involves at least three photons to end in a one-photon peak.

PACS number(s): 42.50.Hz, 33.80.Gj, 33.80.Wz, 34.50.Rk

I. INTRODUCTION

The technological possibility to reach large radiation field intensities with short-pulsed lasers has directed an increasing amount of experimental and theoretical works to multiphoton dissociation dynamics [1]. Optical nonlinearities arising in the absorption spectrum [2], multiphoton above-threshold dissociation [3–5] (ATD), and the so-called "bond-softening" [3,5,6] and "vibrational-trapping" [7,8] mechanisms related to the deformation undergone by the molecule due to its multiphoton coupling with the laser field are the most challenging subjects that have recently been addressed. Due to its relative simplicity, the dissociation of H_2^+ in laser fields with strengths comparable to internuclear binding energies (i.e., $\simeq 50$ TW/cm^2 for which the Rabi frequency is of the same order of magnitude as the local ionic vibrational frequency) serves as an illustrative example system [3,6]. The frequency domain that is considered corresponds, within reasonable approximation, merely to two electronic states of the ion:

$$H_2^+(1s\sigma_g, v) + n\hbar\omega \rightarrow H_2^+(2p\sigma_u) \rightarrow H^+ + H(1s)\ , \qquad (1)$$

and the resonance enhanced preparation of $H_2^+(1s\sigma_g)$ from the ground state of H_2 via the quasibound EF Rydberg state partially supports the neglect of the rotation-field coupling (the J-conserving approximation).

The ion dissociation spectra exhibit multiple peaks in the kinetic-energy distribution of atomic photofragments spaced by the photon energy [3,4,6]. This is the signature of a fragmentation proceeding through multiphoton transitions initiated by the absorption of more photons than the minimum needed to dissociate. It is in connection with a similar behavior in atoms [i.e., above-threshold ionization (ATI)] [9] that this phenomenon has been termed above-threshold dissociation [4,6]. Theory predicts that following the multiphoton absorption by free-free transitions, the molecule being already in its dissociation continuum, and during the process of falling apart, most of the absorbed energy is returned to the electromagnetic field via stimulated emissions, causing a slowing down of the fragments. A rather surprising fragment kinetic-energy distribution results: higher-energy peaks decrease when the field intensity is increased, favoring more and more stimulated free-free emissions by higher-order radiative couplings. A comprehensive analysis of such situations proceeds through an interpretation of photon-exchange mechanisms between the field and the ion. Several dissociation pathways involving more photons than the minimum number required (say n, such that $n = n_a + n_e$, n_a and n_e being the number of absorbed and emitted photons) may be related with a given final net amount of photons which are actually absorbed (say p, with p the algebraic sum of absorbed and emitted photons $p = n_a - n_e$), leading to the corresponding peak in the photofragment spectrum.

A possible nonperturbative theoretical description of these mechanisms induced by intense fields is the dressed-molecule concept [10] with molecular electronic potential-energy surfaces adiabatically modified by the laser [11,12]. For cw lasers, molecule-field coupled-channel formalisms in a time-independent quantum approach have been used to treat simultaneously radiative

and nonradiative interactions [5,11]. The interpretation of multiphoton exchange mechanisms is attempted by referring to laser-induced adiabatic channels involving all photon-number states introduced through the Floquet analysis [2,12–14]. The situation seems more intricate when short-pulsed lasers are considered. Dynamical calculations, using a time-dependent wave-packet propagation, lead to a time-resolved population analysis on the different potential-energy surfaces. Even if the time-dependent behaviors of relative particle fluxes are again interpreted in terms of the field-dressed adiabatic channels of a stationary theory, this is clearly not a rigorous description. Not only do the field-dressed adiabatic channels (a concept related with a *stationary* theory) have to be considered within a time-dependent picture but also, as has been pointed out by Nguyen Dang *et al.* [15], several mechanisms (single and multiphoton) may be in competition at least in the primary steps of the excitation process where the laser field starts from very low values before reaching its maximum. We have recently shown [6,14] how the dynamical description can be combined with some intensity dependence laws (I^n) to identify the leading dissociation pathway involving, for a net amount of p absorbed photons, a total number of n photons exchanged between the radiative field and the molecule.

The aim of the present work is to reconsider this problem by extracting additional information for the widths of the proton kinetic-energy spectrum peaks. For a class of laser pulses (within some intensity and shape ranges, supporting the approximations to be introduced later), a simple analytical formula is derived for the photodissociation spectrum, in terms of the two parameters (n and p) clarifying the understanding of the fragmentation mechanism as resulting from multiphoton absorption-emission processes. Section II presents the theory leading to the calculation of the photodissociation probability for a given photon frequency (corresponding to a given proton kinetic energy), after the pulse is over. The role played by laser-induced resonances [2] is emphasized and their expansion in terms of the complete Floquet basis, describing the different dissociation mechanisms, is worked out through the matrix elements of the reduced Bloch wave operator [16]. In Sec. III, the different peaks of the recently calculated [6] proton kinetic-energy distribution spectra are analyzed within the scope of the previous theory for ultrashort ($\simeq$20 fs duration) and intense (peak intensity within 3.5×10^{12} to 3.5×10^{14} W/cm^2) pulses. For intensities not exceeding 8.7×10^{13} W/cm^2, additional evidence is obtained with respect to previous interpretations of photon-exchange processes, at least for the two- or three-photon peaks. More subtle results enlightening the bond-softening mechanism arise at higher field strengths.

II. THEORY

The starting point is the energy distribution of the protons resulting from multiphoton absorption above the dissociation threshold of H_2^+ in its ground electronic and vibrational state following Eq. (1). Corresponding spectra that have recently been observed [3] and calculated [4,6] consist of a sequence of peaks separated by the photon energy. In the case of a cw laser, a Lorentzian-like behavior is depicted for these peaks, from which the common total width for the laser-induced resonance monitoring the spectrum can be deduced [4]. As for their relative heights, they are related to the branching ratios (partial widths) between asymptotic channels describing different Floquet blocs. More precisely, these ratios give the relative probabilities to dissociate in the continuum of one of the two electronic states (g or u) with a final net amount of p absorbed photons. As has been mentioned before [6], a completely different situation arises when a pulsed laser is considered. Not only the form of the peaks (which, except for very strong field cases, are Gaussian due to the Gaussian shape of the pulse) changes, but also their spectral widths are much larger as compared with the cw laser case [17] and, even more surprising, they are different, for a given intensity, from one peak to the other. This is to be related with the pulsed character of the laser which delivers several frequencies weighted with different intensities. The purpose of the present work is to outline the validity range of the approximations and assumptions that are invoked to model the proton spectrum and to relate the spectral widths by an appropriate deconvolution to a specific dissociation mechanism proceeding through multiphoton absorption and emission processes (n_a photons absorbed, n_e photons emitted).

A. Spectral expansion of the laser pulse

The electromagnetic field amplitude $E(t)$ is given as a product of a time-dependent shape function $\mathcal{S}(t)$, by an oscillating cosine form, with peak frequency ω_0:

$$E(t)=E_0\mathcal{S}(t)\cos\omega_0 t \ . \tag{2}$$

E_0 is a constant amplitude and $\mathcal{S}(t)$ is taken as a Gaussian envelope:

$$\mathcal{S}(t)=\exp[-(t/\tau)^2] \ . \tag{3}$$

The spectral expansion of the pulse is related to the cosine-Fourier transform of $E(t)$:

$$F(\omega)=\frac{1}{2\pi}\int_{-\infty}^{+\infty}\cos(\omega t)E(t)dt \ , \tag{4}$$

which results in

$$F(\omega)=\frac{E_0}{4\sqrt{\pi}}\tau[e^{-(\omega-\omega_0)^2\tau^2/4}+e^{-(\omega-\omega_0)^2\tau^2/4}] \ , \tag{5}$$

i.e., a function displaying two symmetrical peaks at $\pm\omega_0$ with a common width of τ^{-2}. By assuming

$$\tau\omega_0 \gg \pi \tag{6}$$

(an assumption which is fulfilled in the present work where $\tau\sim10$ fs and $\omega_0\simeq0.138\,18$ a.u.), one can completely neglect the overlap between the two peaks and finally retain, by symmetry arguments, the positive axis for ω, leading to the following spectral expansion:

$$E(t)=\int_0^{\infty}\cos(\omega t)F(\omega)d\omega \ , \tag{7a}$$

with

$$F(\omega)=\frac{E_0}{2\sqrt{\pi}}\tau\exp[-(\omega-\omega_0)^2\tau^2/4]\ . \tag{7b}$$

An equivalent set of relations,

$$E(t)=\int_{-\infty}^{+\infty}e^{i\omega t}\mathcal{S}(\omega)d\omega\ , \tag{8a}$$

with $\mathcal{S}(\omega)$ a symmetrical spectrum given by

$$\mathcal{S}(\omega)=\begin{cases}F(\omega)/2 & \text{for } \omega>0 \qquad (8b)\\ F(-\omega)/2 & \text{for } \omega<0\ , \qquad (8c)\end{cases}$$

presents the possibility to conventionally distinguish between absorption ($\omega<0$) and emission ($\omega>0$) mechanisms. In the following we proceed through a discrete spectral expansion, starting from Eq. (7a) and dividing the total frequency extension $\Delta\omega$ of the peak given by Eq. (7b) (which roughly corresponds to a total *finite* time duration Δt of the order of 10 times τ), into N finite intervals:

$$E(t)=\sum_{j=1}^{N}\cos(\omega_j t)F(\omega_j)\delta\omega\ , \tag{9a}$$

with

$$\delta\omega=\frac{\Delta\omega}{N} \tag{9b}$$

and

$$\omega_j=\omega_0-\frac{\Delta\omega}{2}+(j-1)\delta\omega\ . \tag{9c}$$

By assuming the discretization implied by Eq. (9), we are considering a pulsed laser of spectral expansion $F(\omega)$, as a linear superposition of N cw lasers, each characterized by a frequency ω_j and a field strength of $F(\omega_j)\delta\omega$. With a (monochromatic) cw electromagnetic field, one can directly probe the width of a laser-induced resonance resulting from the dressing of the molecular state with a given frequency. This information can be completely washed out when an ultrashort pulse is used. Actually, such a laser presents a spectral width larger than the one of the resonance to be probed. A photodissociation spectrum displays broadened peaks basically depending on the spectral extension of the laser itself. From a schematic viewpoint, the absorption peak corresponds to a convolution of resonances resulting from the interaction of the ground molecular state dressed by the N cw lasers [of Eq. (9)] tuned on different frequencies (ω_j, $j=1,\ldots,N$) corresponding to different radiative coupling strengths [$F(\omega_j)$, $j=1,\ldots,N$]. It is precisely such multimode laser-induced resonances (or Floquet states) that are considered when describing the final dissociation probability.

B. Dissociation probability in terms of Floquet states

The total molecule-plus-field Hamiltonian is written in a semiclassical operator form as

$$H=H_{\text{mol}}+H_{\text{rad}}+V(t)\ , \tag{10}$$

where H_{mol} is the Born-Oppenheimer molecular Hamiltonian involving only two electronic states (g and u) which are assumed to be uncoupled in field-free conditions, H_{rad} is the Hamiltonian of the electromagnetic (em) field, and $V(t)=\mu E(t)$ is the radiative coupling in semiclassical form given as the product of the transition dipole moment times the em field amplitude. This Hamiltonian, after an appropriate Fourier analysis [Eq. (9)], can be expanded on the basis of field-dressed electronic states leading to a time-independent Floquet Hamiltonian [2,13]. The difference as compared to a standard cw Floquet description is that a multimode representation of the field-dressed states is to be performed [18]. The resulting Floquet Hamiltonian H^F in matrix form is given by an appropriate external sum of N Floquet matrices H_i^F:

$$H^F=H_1^F\oplus H_2^F\oplus\cdots\oplus H_N^F\ , \tag{11}$$

each of the H_i^F being related to the ith mode of the em field (or, equivalently, to the ith laser). For completeness, we recall the standard form for H_i^F [13]:

$$H_i^F=\begin{bmatrix} A_i+(n+2)\hbar\omega_i I & B_i & 0\\ {}^TB_i & A_i+n\hbar\omega_i I & B_i\\ 0 & {}^TB_i & A_i+(n-2)\hbar\omega_i I\end{bmatrix}\ , \tag{12}$$

where the two-dimensional A and B matrices are written as

$$A_i=\begin{bmatrix} -\frac{1}{2}\frac{d^2}{dR^2}+V_g(R) & -\mu(R)F(\omega_i)\delta\omega\\ -\mu(R)F(\omega_i)\delta\omega & -\frac{1}{2}\frac{d^2}{dR^2}+V_u(R)-\hbar\omega_i\end{bmatrix} \tag{13a}$$

and

$$B_i=\begin{bmatrix} 0 & 0\\ -\mu(R)F(\omega_i)\delta\omega & 0\end{bmatrix}\ . \tag{13b}$$

I is the two-dimensional identity matrix, T indicates the transpose, $V_g(R)$ and $V_u(R)$ are the potential energies of g and u states, and R designates the dissociative nuclear coordinate.

An asymptotic zero-order basis set $\{|\beta,k_1,k_2,\ldots,k_N\rangle\}$ can be defined for H^F after the pulse is over (i.e., in the absence of radiative coupling). β represents either a vibrational bound level of the ground

electronic state g or a vibrational continuum state which is either associated with the dissociative part of g or u electronic states. k_i $(i=1,\ldots,N)$ specifies the actual number of photons of frequency ω_i in the ith mode of the field (which corresponds to the ith laser in our discretized scheme). This number is given an algebraic specification:

$$k_i = n_{e_i} - n_{a_i} , \tag{14}$$

such that k_i is related to a difference of emitted (n_{e_i}) and absorbed (n_{a_i}) photons during the process. A negative value for k_i indicates a multiphoton process which ends up with a final balance of absorption. The initial molecule-plus-field state is one of the vectors of the basis set denoted by $|\alpha,0,0,\ldots,0\rangle$, where α designates the vibrationless level of the ground electronic state (g, $v=0$, $J=1$), without any photon on the N modes of the field.

The diagonalization of the Floquet Hamiltonian [Eq. (11)] leads to another complete basis set of vectors $\{|L_{\beta,k_1,k_2,\ldots,k_N}\rangle\}$ which includes both the field-induced resonances and the scattering-state eigenvectors of H^F:

$$H^F|L_{\beta,k_1,k_2,\ldots,k_N}\rangle = \varepsilon_{\beta,k_1,k_2,\ldots,k_N}|L_{\beta,k_1,k_2,\ldots,k_N}\rangle . \tag{15}$$

The label $(\beta,k_1,k_2,\ldots,k_N)$ indicates that the corresponding vector $|L\rangle$ proceeds from the state $|\beta,k_1,k_2,\ldots,k_N\rangle$ with an adiabatically switched radiative coupling.

Following Chu's derivation [18], we can write the probability of a transition from the initial state α to a final state β by absorbing a total amount of p photons during a finite duration Δt of the pulse as

$$P^p_{\beta\alpha}(\Delta t)=\sum_{\{k_1,\ldots,k_N\}} |\langle\beta^\dagger,k_1,k_2,\ldots,k_N|U(\Delta t)|\alpha,0,0,\ldots,0\rangle|^2 , \tag{16a}$$

where the photon numbers k_i satisfy

$$\sum_{i=1}^{N} k_i = -p \tag{16b}$$

and

$$U(\Delta t)=\exp(-i/\hbar\, H^F\Delta t) \tag{17}$$

is the evolution operator under the action of the Floquet Hamiltonian. In practical computations using grids of finite extension [the discretized variable representative (DVR) [19] in the present case], an asymptotic optical potential is introduced, such that the resonance and scattering eigenfunctions are square integrable. The consequence is the biorthonormality of the vectors $|\beta\rangle$ and $|L\rangle$, which is indicated by the $\dagger$ sign in Eq. (16).

$$P^p_{\beta\alpha}(\Delta t)=\sum_{\{k_1,\ldots,k_N\}}\left|\sum_{\{\gamma,l_1,\ldots,l_N\}}\langle\beta^\dagger,k_1,\ldots,k_N|L_{\gamma,l_1,\ldots,l_N}\rangle\langle L^\dagger_{\gamma,l_1,\ldots,l_N}|\alpha,0,0,..,0\rangle\exp(-i/\hbar\,\varepsilon_{\gamma,l_1,\ldots,l_N}\Delta t)\right|^2 . \tag{18}$$

The most drastic approximation of our approach consists in retaining only resonances (or ignoring scattering states) in the second $\sum$ involved in Eq. (18). Such an approximation, which can numerically be checked, has a validity domain that basically depends on the following laser characteristics: (i) not very strong field intensities and (ii) smooth pulse shape (adiabatic switching on and off of the laser).

If, in addition, there is no resonance overlapping (as in the case of intermediate radiative couplings), the major contribution to the sum of Eq. (18) is provided by but one resonance, i.e., $|L_{\alpha,0,\ldots,0}\rangle$ related to the initial bound state $|\alpha,0,\ldots,0\rangle$, progressively modified by adiabatically switching the em field on from $t=-\infty$ to $t=0$. Within these assumptions, Eq. (18) can be rewritten in an oversimplified, but tractable, way as

$$P^p_{\beta\alpha}(\Delta t)\simeq C_\alpha(\Delta t)\sum_{\{k_1,\ldots,k_N\}}|\langle\beta^\dagger,k_1,\ldots,k_N|L_{\alpha,0,\ldots,0}\rangle|^2 , \tag{19a}$$

where

$$C_\alpha(\Delta t)=\exp\{2\Delta t/\hbar\,\mathrm{Im}(\varepsilon_{\alpha,0,\ldots,0})\}|\langle L^\dagger_{\alpha,0,\ldots,0}|\alpha,0,\ldots,0\rangle|^2 . \tag{19b}$$

$\mathrm{Im}(\varepsilon_{\alpha,0,\ldots,0})$ is negative as usual, but in a discretized representation of the pulse, Δt has an assigned finite value of the order of τ, such that the exponential factor remains nonzero, and is actually close to unity for very narrow resonances. The physical picture that arises from Eqs. (18) and (19) is precisely the one that has already been invoked in previous works [11,20], i.e., the initial state $|\alpha,0,\ldots,0\rangle$ is expanded on field-induced resonances $|L_{\gamma,l_1,\ldots,l_N}\rangle$ with appropriate weighting coefficients: $\langle L_{\gamma,l_1,\ldots,l_N}|\alpha,0,\ldots,0\rangle$. These resonances evolve as eigenvectors of the total multimode time-independent

Floquet Hamiltonian during the laser pulse and are projected on asymptotic Floquet channels $|\beta,k_1,\ldots,k_N\rangle$ describing the composite final molecular state β which is reached with the corresponding total amount of absorbed or emitted photons on each mode. Equation (19) refers, more specifically, to cases where the weighting coefficients are approximatively given by

$$\langle L^{\dagger}_{\gamma,l_1,\ldots,l_N}|\alpha,0,\ldots,0\rangle \simeq \delta_{\alpha\gamma}\delta_{Ol_1}\cdots\delta_{Ol_N} . \tag{20}$$

It has to be stressed that in intermediate field-strength conditions, leading to negligible resonance overlapping, such cases are rather common [21].

The evaluation of partial dissociation probabilities requires an appropriate summation over all final molecular states. The dissociation probability for a final amount of p absorbed photons is thus given by

$$P_p \simeq C_\alpha(\Delta t)\sum_{\beta}\sum_{\{k_1,\ldots,k_N\}}|\langle\beta^{\dagger},k_1,\ldots,k_N|L_{\alpha,0,\ldots,0}\rangle|^2 . \tag{21a}$$

The sum over β concerns all the discretized vibrational continua of g (for even p) or u (for odd p) states and the k_i's which are retained fulfill the condition displayed by Eq. (16b). A clear interpretation of Eqs. (21) in terms of the photodissociation spectrum is based on two assumptions: (i) the peaks representing a final amount of p absorbed photons (distant from ω_0, the peak frequency of the laser) are well separated, which is normally expected with a laser bandwidth less than ω_0 [cf. Eq. (6)], and (ii) each p-photon peak is related to but one dissociation mechanism, implying n total photons ($n \geq p$) absorbed and emitted during the process.

These conditions being fulfilled, P_p [Eqs. (21)] represents the integrated area under the p-photon peak (cf. Fig. 6, Ref. [6]), the branching ratio between p_1- and p_2-photon peaks being merely P_{p_1}/P_{p_2}.

A detailed, energy-resolved information which leads to the spectral width of a given p-photon peak can be obtained by further restricting the summation in Eq. (21a). Among all combinations of k_i leading to Eq. (16b), the ones which are retained correspond to a final energy Ω (with Ω varying around a central value of $p\omega_0$). With this additional constraint

$$\sum_{i=1}^{N} k_i\omega_i = \Omega , \tag{21b}$$

the shape (and, consequently, the width) of the p-photon peak (cf. Fig. 6, Ref. [61]) can be reached, in terms of a given dissociation pathway (i.e., the total number n of photons):

$$P(\Omega) \propto \sum_{\beta}\sum_{\{k_1,\ldots,k_N\}}{}' |\langle\beta^{\dagger},k_1,\ldots,k_N|L_{\alpha,0,\ldots,0}\rangle|^2 , \tag{21c}$$

where $\sum'$ refers to conditions displayed by Eqs. (16b) and (21b).

The constraint of a total number of n photons involved in the dynamics cannot be related to a particular choice of k_i's which are the final field occupation numbers. The way in which this condition is fulfilled is clarified in Sec. II C.

C. Photodissociation spectrum

The Bloch wave operator formalism [16] appears to be a convenient and direct way to calculate the projections of $|L_{\alpha,0,\ldots,0}\rangle$ on the zero-order basis $\{|\beta,k_1,\ldots,k_N\rangle\}$ which are the main ingredients building up Eqs. (21a) and (21c). A detailed description of this method has recently been given [6,16]. A one-dimensional subspace S_0 containing the initial vector $|\alpha,0,\ldots,0\rangle$ is defined with its associated projector

$$P_0 = |\alpha,0,\ldots,0\rangle\langle(\alpha,0,\ldots,0)^{\dagger}|$$

and a normalization such that

$$\langle\alpha^{\dagger},0,\ldots,0|L_{\alpha,0,\ldots,0}\rangle = 1 . \tag{22}$$

The so-called reduced wave operator X controls transitions from S_0 to its complementary subspace S_0^+ built up by the vectors $\{|\beta,k_1,\ldots,k_N\rangle\}$. A column of X, specified by the particular choice of S_0 (i.e., of the initial vector $|\alpha,0,\ldots,0\rangle$), is an eigenvector of H^F, normalized according to Eq. (22). So the scalars $\langle\beta,k_1,\ldots,k_N|L_{\alpha,0,\ldots,0}\rangle$ are nothing but the matrix elements of X. They are obtained at an arbitrarily high perturbation order, using the following iterative scheme [16]:

$$X = \lim_{M\to\infty} X^{(M)} , \tag{23a}$$

$$X^{(0)} = 0 , \tag{23b}$$

$$X^{(M)} = X^{(M-1)} + \sum_j |j\rangle\langle\alpha| \left[\frac{\langle j|H^{IM)}|\alpha\rangle}{\langle\alpha|H^{(M)}|\alpha\rangle - \langle j|H^{(M)}|j\rangle} \right] , \tag{23c}$$

$$H^{(M)} = (1-X^{(M-1)})H(1+X^{(M-1)}) , \tag{23d}$$

where condensed notations are introduced, i.e., H for H^F, $|\alpha\rangle$ for the vector $|\alpha,0,\ldots,0\rangle$ of S_0 and $|j\rangle$ for the vectors $|\beta,k_1,\ldots,k_N\rangle$ of S_0^+. The first two steps of the iteration

$$[X^{(1)}]_{j\alpha} = H_{j\alpha}/(H_{\alpha\alpha}-H_{jj}) , \tag{24a}$$

$$[X^{(2)}]_{j\alpha} \simeq [X^{(1)}]_{j\alpha} + \sum_{m\,(\neq j)} H_{jm}H_{m\alpha}/(H_{\alpha\alpha}-H_{jj})(H_{\alpha\alpha}-H_{mm}) - \sum_k H_{j\alpha}H_{\alpha k}H_{k\alpha}/(H_{\alpha\alpha}-H_{jj})^2(H_{\alpha\alpha}-H_{kk}) , \tag{24b}$$

where second-order ac Stark shifts are neglected in the denominators of Eq. (24b)], lead to the following general considerations, as the structure of higher-order terms are

completely similar.

(i) Due to the optical potential, H_{jj} is complex while $H_{\alpha\alpha}$ is still real; energy poles are thus avoided, although some quasidegenerate states (α,m) may play a major part in the calculation. In addition, the denominators are built up from diagonal elements of H representing the molecule-plus-field energies. Within the assumption of a relatively narrow bandwidth pulse [Eq. (6)], the energy differences between the n modes can be neglected such that the dependence remains only on the total number of photons.

(ii) The numerators appear to be products of nondiagonal terms of H representing radiative couplings between molecule-plus-field states differing by one photon and corresponding to a given mode of the field. More precisely, in order to describe a dissociation pathway involving a total amount of n photons, one has to perform the iterations [Eq. (23)] up to $M=n$. For $M=2$, for instance, the first two terms in the right-hand side of Eq. (24) are, respectively, the complete one- and two-photon contributions, the last term being a partial contribution of the three-photon process.

Finally, for an n-photon process involving an intermediate field intensity, only contributions of products of n off-diagonal terms of H are retained when calculating $X^{(n)}$. $P(\Omega)$ [Eq. (21c)] can be approximated by

$$P(\Omega)\simeq\sum_{\beta}\sum_{\{k_1,\ldots,k_N\}}{}'\,x_{\beta\alpha}\left|\left\langle\beta^{\dagger},k_1,\ldots,k_N\left|\prod_n H^F_{\rm nd}\right|\alpha,0,\ldots,0\right\rangle\right|^2, \tag{25}$$

where $H^F_{\rm nd}$ means the nondiagonal elements of H^F (radiative couplings) and the products symbolized by $\prod_n$ contain n terms. It has to be emphasized that the specific signature of a finite-duration pulse (by comparison with a cw laser) is the dependence with respect to the different field modes. Such a difference having been neglected in the denominators of Eqs. (23), a proportionality factor $x_{\beta\alpha}$ is merely introduced in Eq. (25). All photon-mode dependence is related with the matrix element of $\prod_n H^F_{\rm nd}$.

An explicit expression for a nondiagonal matrix element of H^F can be given as

$$\langle\beta^{\dagger},k_1,\ldots,k_N|H^F|\gamma,l_1,\ldots,l_N\rangle=\langle\beta^{\dagger}|\mu|\gamma\rangle\sum_{i=-N}^{N}\mathcal{S}(\omega_i)\delta\omega\langle k_1,\ldots,k_N|e^{i\omega_i t}|l_1,\ldots,l_N\rangle\ . \tag{26}$$

This is because β and γ states differ by a unique photon of a mode i, an absorption (or emission) corresponding to a negative (or positive) i. The next step of the calculation is the evaluation of the field matrix elements $\langle k_1,\ldots,k_N|e^{i\omega_j t}|l_1,\ldots,l_N\rangle$, which are either 0 or 1. The cases where they differ from 0 correspond to the two following simultaneously fulfilled conditions:

$$l_{|i|}=k_{|i|}+\mathrm{sgn}i\quad(\mathrm{sgn}i=\pm1)\quad\text{for } j=i \tag{27a}$$

or

$$l_{|j|}=k_{|j|}\quad\text{for } j\neq i\ . \tag{27b}$$

By combining Eqs. (25)–(27), one can write, for an n-photon process

$$P(\Omega)\simeq\sum_{\beta}\bar{x}_{\beta\alpha}\sum_{\{k_1,\ldots,k_N\}}{}'\left|\left\{\left[\sum_{i_1=-N}^{N}\mathcal{S}(\omega_{i_1})\delta\omega\right]\cdots\left[\sum_{i_n=-N}^{N}\mathcal{S}(\omega_{i_n})\delta\omega\right]\right\}\right|^2. \tag{28}$$

It is to be pointed out that, as a consequence of Eqs. (27), among all the laser modes involved in the sums over $i_1, i_2,\ldots,i_n$, the ones which are retained correspond precisely to those which lead to the particular state $(k_1,k_2,\ldots,k_N)$ when starting from the initial state $(0,0,\ldots,0)$. After taking the limit of Eq. (28) for large N (which results in the transformation of the discrete sums into integrals) and performing an appropriate change of variable by referring all frequencies to Ω corresponding to the total energy of the final state $(k_1,\ldots,k_N)$, one gets

$$P(\Omega)\simeq Q_\alpha\left|\int_{-\infty}^{+\infty}d\omega_n\mathcal{S}(\Omega-\omega_n)\int_{-\infty}^{+\infty}d\omega_{n-1}\mathcal{S}(\omega_n-\omega_{n-1})\cdots\int_{-\infty}^{+\infty}d\omega_1\mathcal{S}(\omega_2-\omega_1)\mathcal{S}(\omega_1)\right|^2. \tag{29}$$

The ω_i's are now defined as field-state frequencies rather than transition frequencies between these states and the proportionality coefficient Q_α results from the sum over all molecular states β. The product of integrals in the right-hand side (r.h.s.) of Eq. (29) can be given a compact single integral form. $\mathcal{S}(\omega)$ being the Fourier transform of $E(t)$, as indicated in Eq. (8a), the convolution theorem applied at nth order results in

$$\mathcal{F}\left\{\int_{-\infty}^{+\infty}d\omega_n\mathcal{S}(\Omega-\omega_n)\cdots\int_{-\infty}^{+\infty}d\omega_{n-1}\mathcal{S}(\omega_2-\omega_1)\mathcal{S}(\omega_1)\right\}$$

$$=[E(t)]^n \tag{30a}$$

and, reciprocally,

$$\int_{-\infty}^{+\infty} d\omega_n \mathcal{S}(\Omega-\omega_n)\cdots\int_{-\infty}^{+\infty} d\omega_1 \mathcal{S}(\omega_2-\omega_1)\mathcal{S}(\omega_1)$$

$$=\int_{-\infty}^{+\infty} e^{-i\Omega t}[E(t)]^n dt \ . \quad (30b)$$

By combining Eqs. (2) and (3), one gets

$$[E(t)]^n=E_0^n \cos^n(\omega_0 t)\exp\left[-\frac{t^2}{(\tau/\sqrt{n})^2}\right], \quad (31)$$

where $\cos^n(\omega_0 t)$ can be expanded in terms of a power sum:

$$\cos^n(\omega_0 t)=2^{-n}\sum_{k=0}^{n}\binom{n}{k}\exp[i(2k-n)\omega_0 t] \ , \quad (32)$$

$\binom{n}{k}$ indicating the binomial coefficients.

Considering that the final frequency $\Omega\sim p\omega_0$ and that the different p-photon peaks are well separated in the spectrum [Eq. (6)], the major contribution to the integral on the r.h.s. of Eq. (30b) is provided by a term in the expansion [Eq. (32)] corresponding to

$$2k-n=p \ . \quad (33)$$

All other k values leading to high-frequency oscillations being merely neglected, the r.h.s. of Eq. (30b) is approximated by

$$\int_{-\infty}^{+\infty} e^{-i\Omega t}[E(t)]^n dt \simeq \exp[-(\Omega-p\omega_0)^2(\tau/\sqrt{n})^2/4] \ . \quad (34)$$

The Ω dependence of the spectrum is then obtained from Eqs. (29), (30), and (34):

$$P(\Omega)\propto \exp[-\tfrac{1}{2}(\tau/\sqrt{n})^2(\Omega-p\omega_0)^2] \ . \quad (35)$$

Equation (35) is the final result of this analysis and provides, within the validity range of the assumptions that have been discussed, a Gaussian-type behavior for the peaks of the photodissociation spectrum using a pulsed laser (Gaussian pulse of peak frequency ω_0 and pulse duration τ). Peaks are located at $p\omega_0$ (p being the final amount of absorbed photons) and their full widths at half maximum (FWHM) are proportional to the square root of n (the total number of exchanged photons):

$$\Gamma_n=(8\ln 2)^{1/2}\sqrt{n}/\tau \ . \quad (36)$$

III. RESULTS

The analytic expression for the photodissociation spectrum obtained in Sec. II [Eq. (35)] is used for the interpretation of proton kinetic-energy distributions resulting from H_2^+ photodissociation [Eq. (1)].

Figures 1 and 2 display proton relative populations as a function of their kinetic energy (the so-called proton kinetic-energy spectra) for two particular field intensities, namely, $I=3.5\times10^{12}$ and 5.6×10^{13} W/cm^2, corresponding to intermediate and strong regimes. The laser is tuned on a peak frequency $\omega_0=30\,333$ cm^{-1} (or a wavelength $\lambda_0=329.67$ nm) and delivers Gaussian-shaped pulses of duration $2\tau\simeq20$ fs.

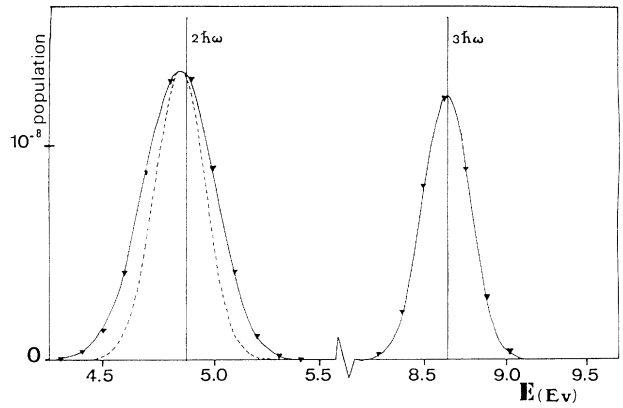

FIG. 1. Proton relative populations as a function of the total kinetic energy resulting from 329-nm dissociation of H_2^+ at 3.5×10^{12} W/cm^2. The thin vertical lines indicate the kinetic energies of the three- or two-photon processes. The solid triangles correspond to the full time-dependent calculation of Ref. [6]. The analytical spectrum of the present work [Eq. (35)] is plotted using either the solid line (for the most appropriate values of n, the number of photons of the leading mechanism, i.e., $n=3$, or $n=4$ for the three- or two-photon peaks, respectively) or the dashed line (for other processes, i.e., $n=2$ for the two-photon peak). A scaling factor ($\times10$) is introduced for the two-photon peak.

Basically, each spectrum exhibits two or three peaks roughly separated by the photon frequency $\hbar\omega_0$. The two fragments (i.e., H and H^+) of equal masses separate in the center-of-mass reference frame with a quantized energy of $p\hbar\omega_0$ following an absorption of p photons ($p=1$, 2, or 3). Superimposed on these spectra are the distributions resulting from Eq. (35), with the most appropriate values of n.

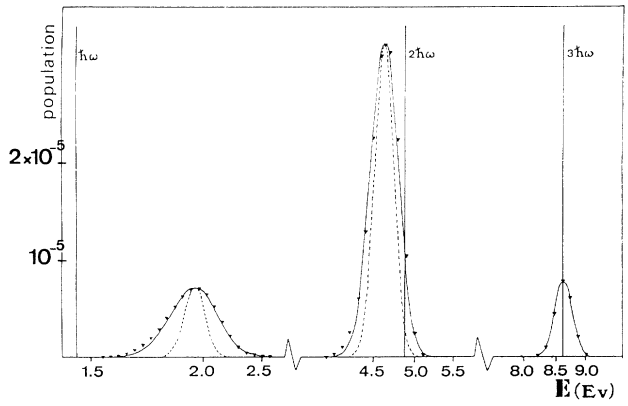

FIG. 2. Same as for Fig. 1, with a stronger intensity of 5.6×10^{13} W/cm^2. The thin vertical lines indicate the kinetic energies of the three-, two-, and one-photon processes. The solid curves correspond to three-photon ($n=3$), four photon ($n=4$), and five photon ($n=5$) leading mechanisms underlying the three-, two-, and one-photon peaks, respectively. The dashed curves illustrate alternative pathways for the two- and one-photon peaks [i.e., two- ($n=2$) and one- ($n=1$) photon leading mechanisms, respectively] corresponding to a less accurate fit with respect to the full time-dependent calculation.

Several remarks are in order.

(i) For the intensities under consideration, the full quantum calculated peaks [6] show a symmetrical behavior that can well be reproduced by the Gaussian shape of the analytic expression (35). At higher intensities ($I > 2\times10^{14}$ W/cm^2), the agreement is less satisfactory.

(ii) The three-photon peaks are well located at $3\hbar\omega_0$, as expected; the two-photon peaks ar very slightly redshifted, remaining, however, in reasonable agreement with Eq. (35) (0.224 eV for $I = 5.6\times10^{13}$ W/cm^2 in Fig. 2; for comparison, this shift is only 0.0275 eV for $I = 3.5\times10^{12}$ W/cm^2), but a larger shift affects the one-photon peak of Fig. 2 which is positioned at higher energies than $\hbar\omega_0$.

(iii) The most relevant information concerns spectral widths. For the two intensity regimes, the three-photon peaks are reproduced within excellent accuracy by referring to a mechanism involving three-photon exchange ($n = 3$) ending up in three-photon net absorption ($p = 3$). The two-photon peaks, in turn, are clearly better reproduced by taking ($n = 4$, $p = 2$) rather than ($n = 2$, $p = 2$), indicating a mechanism which involves a three-photon absorption followed by an emission which occurs during the dissociation process itself. As for the one-photon peak, at the precise intensity of Fig. 2, it seems that an acceptable fit can be obtained by retaining ($n = 5$, $p = 1$) which constitutes a rough indication for a three-photon absorption followed by successive emissions of two photons. This situation is, however, accidental and does not hold for higher intensities.

A partial interpretation that can be inferred is that for intermediate intensities and for the three- and two-photon peaks, the assumptions made in Sec. II are adequately met and a unique mechanism for the multiphoton process can be proposed from the analysis of spectral widths, as for the one-photon peak, this simple scheme does not hold, presumably because several multiphoton processes, each involving a different number of photons $n_1, n_2, \ldots$, end up with a final net balance of one absorbed photon. Very recently, at least two of these mechanisms ("above-threshold dissociation" after absorption of three and emission of two photons, i.e., $n = 5$, $p = 1$, or "bond softening" by potential-energy-barrier lowering, i.e, $n = 1$, $p = 1$) have been devised [6].

A more refined analysis is presented in Fig. 3. For all field strengths under consideration, the spectral widths of the one-, two-, and three-photon peaks ($p = 1$, 2, and 3), as taken from [6], are displayed together with their (FWHM) values resulting from Eq. (36) when n is varied from 3 to 8. An inspection of this figure together with Fig. 4 taken from Ref. [6] and displaying the relevant field-dressed adiabatic potentials resulting from the diagonalization of the radiative coupling leads to the following conclusions.

(i) For intensities up to 1.4×10^{13} W/cm^2, the three-photon peak dominates the spectrum, and it shows non-negligible values for $I < 10^{14}$ W/cm^2. Within this intensity range, it can clearly be asserted that the three-photon peaks ($p = 3$) correspond to an above-threshold dissociation following the absorption of three photons ($n = 3$). This is illustrated in Fig. 4 where, starting from channel $|1s\sigma_g, n+1\rangle$, the process following a diabatic jump ends up in channel $|2p\sigma_u, n-2\rangle$.

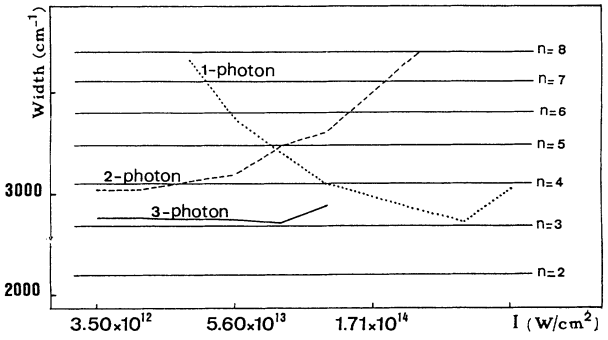

FIG. 3. Full width at half maximum of the three- ($p = 3$), two- ($p = 2$), and one- ($p = 1$) photon peaks of the proton kinetic-energy spectrum resulting from 329-nm dissociation of H_2^+ at different field intensities as calculated in Ref. [6]. The solid, dashed, and dotted lines correspond to the three- ($p = 3$), two- ($p = 2$), and one- ($p = 1$) photon peaks, respectively. Also indicated by thin horizontal lines are the values of the widths as extracted from the analysis of the present work [Eq. (36)] for different values of the total number of exchanged photons ($n = 3$ to 8). A coincidence between one of the three curves ($p = 1$, 2, or 3) and the horizontal lines is an indication for the leading mechanism (n,p).

(ii) The two-photon peaks start with relatively low heights at $I = 3.5\times10^{12}$ W/cm^2, increase progressively, and dominate the spectrum at $I = 5.6\times10^{13}$ W/cm^2, before decreasing. A mechanism involving the absorption of three photons followed by the emission of a fourth photon ($n = 4$) can be proposed at least for I up to 5.6×10^{13} W/cm^2. This can be envisioned in Fig. 4 where an adiabatic jump from channel $|2p\sigma_u, n-2\rangle$ to channel $|1s\sigma_g, n-1\rangle$ occurs after the initial three-photon absorption and while the system is dissociating. For higher intensities, a larger number of photons ($n = 8$, for instance,

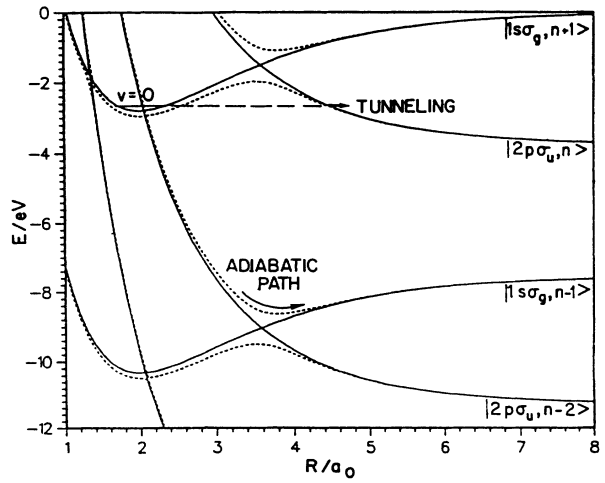

FIG. 4. Potential-energy curves of H_2^+ dressed by a 329-nm wavelength laser. Solid curves, diabatic (unperturbed) $1s\sigma_g$ and $2p\sigma_u$ states shifted by the corresponding photon energy $n\hbar\omega$; dotted curves, adiabatic potentials for $I = 1.4\times10^{13}$ W/cm^2.

for $I=2.24\times10^{14}$ W/cm^2) are exchanged between the field and the molecule resulting in very large spectral widths.

(iii) The one-photon peaks dominate the spectrum for intensities exceeding 8×10^{13} W/cm^2. For $I=8.75\times10^{13}$ W/cm^2, the spectral-width analysis leads to a five-photon process ($n=5$), which according to a Franck-Condon type of argument can be decomposed into an initial absorption of three photons followed by the subsequent emission of two photons. The succession of events, as can be followed schematically from Fig. 4, is thus

$$|1s\sigma_g,n+1\rangle\rightarrow|2p\sigma_u,n-2\rangle \rightarrow|1s\sigma_g,n-1\rangle\rightarrow|2p\sigma_u,n\rangle\ .$$

At higher field strengths, the order of the multiphoton exchange mechanism is decreasing, reaching for $I>2\times10^{14}$ W/cm^2, the value $n=3$.

The first two points (i) and (ii) support and complete the conclusions previously drawn in Ref. [6]. Point (iii) suggests the possibility of a slightly different interpretation. The aforementioned interpretative scheme is a multiphoton mechanism for intensities up to 10^{14} W/cm^2, which then competes with a single-photon process due to considerable local modification of potential energies by the presence of the laser (lowering of the adiabatic barrier resulting from the interaction of diabatic channels $|1s\sigma_g,n+1\rangle$ and $|2p\sigma_u,n\rangle$, as indicated by the dotted line of Fig. 4, and leading to the so-called bond softening). Such an interpretation is, of course, plausible, but still remains beyond the scope of the present analysis based on the hypothesis of a unique photon-exchange mechanism (one given n) responsible for a given p-photon peak. An alternate picture which rises is the penetration of the lowering potential barrier (the dotted line of Fig. 4), but after two reflections (absorption-emission-absorption, i.e., $n=3$) instead of a single jump (absorption, i.e., $n=1$). A somewhat similar discussion is presented in a recent work by one of us (O.A.) [14], but referring to a cw laser experiment. Although in intermediate to strong field regimes, the three- and four-photon mechanisms are clearly identified as the leading interpretation for the three- and two-photon peaks, respectively, the one-photon peak cannot be attributed to a unique photon-exchange mechanism: it is rather to be viewed as a superposition of a variety of multiphoton processes.

IV. CONCLUSION

In conclusion, we would like to emphasize that, within the framework of some reasonable assumptions and approximations, the spectral widths of a multiphoton dissociation spectrum, obtained by the use of a short and intense laser pulse, can be analyzed through a very simple analytical formula. The complete history of the dissociation process, in terms of the numbers of absorbed and emitted photons, is drawn and used as an interpretative tool which completes other measurements or dynamical calculations.

More precisely, the *assumptions* concern laser and spectrum characteristics. They can be summarized as follows: (i) field intensities have to range in the intermediate to strong regime, i.e., 10^{12} W/cm$^2<I<10^{14}$ W/cm^2; (ii) the pulse must not exhibit strong temporal variations (adiabatic switching); (iii) the pulse bandwidth must not be very large (or not of too short duration); and (iv) the spectrum has to present well-separated p-photon absorption peaks associated with a unique multiphoton mechanism involving a total amount of n photons.

These assumptions basically support the following *approximations.*

(i) A unique, well-isolated, field-induced resonance is selected and retained, through which the fragmentation proceeds. The validity range of this approximation is related to the intermediate field strength and smooth pulse switching [assumptions (i) and (ii) above].

(ii) The role played by different laser modes is neglected when calculating the field-dressed energy differences in the denominators of the reduced Bloch wave operators [in relation with assumption (iii) above].

(iii) Referring to well-separated peaks in the spectrum [assumptions (iv) and (iii) above], a unique term, corresponding to the lowest oscillation frequency in the expansion of $\cos^n\omega_0 t$ (part of the temporal behavior of the electromagnetic field), is retained for each p-photon peak.

The analytic formula which is obtained relates the spectral width of a p-photon peak to a given n-photon mechanism, thus providing a more quantitative basis to previous interpretations of the dissociation dynamics of H_2^+ in terms of population transfers between adiabatic Floquet channels. For intermediate field intensities, the conclusions are consistent with recent works, especially for the three- and two-photon peaks resulting, reciprocally, from three-photon absorption or three-photon absorption followed by one-photon emission processes. At higher intensities, the potential-energy curves undergo large-scale modifications leading to the so-called bond softening by energy-barrier lowering. The one-photon peaks correspond to a three-photon absorption-emission-absorption mechanism which can be interpreted as a tunneling through such barriers after two reflections.

ACKNOWLEDGMENTS

This work is supported by Cooperation France-Québec ESR, Contract No. 010392. A grant of computing time from the Conseil Scientifique du Centre de Calcul Vectoriel pour le Recherche (C.C.V.R.) is also gratefully acknowledged.

[1] P. B. Corkum, IEEE J. Quantum Electron. **21**, 216 (1985); C. Cornaggia, D. Normand, J. Morellec, G. Mainfray, and C. Manus, Phys. Rev. A **34**, 207 (1986); J. Verschuur, L. Noordam, and H. van Linden van den Heuvell, *ibid.* **40**, 4383 (1989); *Coherence Phenomena in Atoms and Molecules in Laser Fields*, Vol. B287 of *Nato Advanced Study Institute, Series B: Physics*, edited by A. D. Bandrauk and S. C. Wallace (Plenum, New York, 1992).

[2] X. He, O. Atabek, and A. Giusti-Suzor, Phys. Rev. A **38**, 5586 (1988).

[3] A. Zavriyev, P. H. Bucksbaum, H. G. Muller, and D. W. Schumacher, Phys. Rev. A **42**, 5500 (1990); P. H. Bucksbaum, A. Zavriyev, H. G. Muller, and D. W. Schumacher, Phys. Rev. Lett. **64**, 1883 (1990); B. Yang, M.Saeed, L. F. Dimauro, A. Zavriyev, and P. H. Bucksbaum, Phys. Rev. A **44**, R1458 (1991).

[4] A. Giusti-Suzor, X. He, O. Atabek, and F. H. Mies, Phys. Rev. Lett. **64**, 515 (1990).

[5] A. D. Bandrauk, E. Constant, and J. M. Gautheir, J. Phys. II (France) **1**, 1033 (1991).

[6] G. Jolicard and O. Atabek, Phys. Rev. A **46**, 5845 (1992).

[7] A. D. Bandrauk and M. L. Sink, J. Chem. Phys. **74**, 1110 (1981); A. D. Bandrauk and G. Turcotte, *ibid.* **77**, 3867 (1982).

[8] A. Giusti-Suzor and F. H. Mies, Phys. Rev. Lett. **68**, 3869 (1992).

[9] P. Agostini, F. Fabre, G. Mainfray, G. Petite, and N. Rahman, Phys. Rev. Lett. **42**, 1127 (1979); R. M. Potvliege and R. Shakeshaft, Phys. Rev. A **38**, 4597 (1988); C. Cohen-Tannoudji, in *Frontiers in Laser Spectroscopy,* edited by R. Balian, S. Haroche, and S. Liberman (North-Holland, Amsterdam, 1977), Vol. 1, pp. 3–104.

[10] T. F. George, I. H. Zimmerman, J. M. Yuan, J. R. Laing, and P. L. Devries, Acc. Chem. Res. **10**, 449 (1977); T. F. George, J. Phys. Chem. **86**, 10 (1982).

[11] A. D. Bandrauk and O. Atabek, Adv. Chem. Phys. **73**, 823 (1989).

[12] X. He, O. Atabek, and A. Giusti-Suzor, Phys. Rev. A **42**, 1585 (1990).

[13] S. I. Chu, J. Chem. Phys. **75**, 2215 (1981).

[14] M. Chrysos, O. Atabek, and R. Lefebvre, Phys. Rev. A **48**, 3855 (1993).

[15] H. Abou-Rachid, T. T. Nguyen-Dang, R. K. Chaudhury, and X. He, J. Chem. Phys. **97**, 5497 (1992).

[16] G. Jolicard, J. Chem. Phys. **90**, 2320 (1989); G. Jolicard and J. Humbert, Comput. Phys. Commun. **63**, 216 (1991); G. Jolicard and G. D. Billing, Chem. Phys. **149**, 261 (1991).

[17] For instance, at $I=1.4\times10^{13}$ W/cm^2 ($\lambda=329.7$ nm), the spectral width of the two-photon peak is 1750 times larger than the total width of a cw-laser-induced resonance situated at the corresponding energy (see Fig. 3 of Ref. [4] and Fig. 6 of Ref. [6]).

[18] S. I Chu, Adv. Chem. Phys. **73**, 739 (1989).

[19] J. C. Light, I. P. Hamilton, and J. V. Lill, J. Chem. Phys. **82**, 1400 (1985); J. T. Muckerman, Chem. Phys. Lett. **173**, 200 (1990).

[20] S. Miret-Artès, O. Atabek, and A. D. Bandrauk, Phys. Rev. A **45**, 8056 (1992).

[21] G. Jolicard, J. Killingbeck, P. Durand, and J. L. Heully, J. Chem. Phys. (to be published).